Pergamon

Cement and Concrete Research 30 (2000) 1535–1542

CEMENT AND CONCRETE RESEARCH

The distributions of bound sulfates and chlorides in concrete subjected to mixed NaCl, $MgSO_4$, Na_2SO_4 attack

P.W. Brown[a,*], Steven Badger[b]

[a]*Department of Materials Science and Engineering, Penn State University, 136 M.R.L., University Park, Hershey, PA 16802, USA*
[b]*R.J. Lee Group, Monroeville, PA 15146, USA*

Received 1 July 1998; accepted 3 June 2000

Abstract

This article describes phenomena typical of those observed in concrete flatwork exposed to sulfate soils, which had been undergoing sulfate attack. In particular, the spatial distribution of sulfate-containing phases as a result of the ingress of ground water is discussed. Intrusion of sulfate from ground water resulted in the formation of zones of ettringite and gypsum. These zones formed in response to the sulfate gradient. Because the high permeabilities are typical of the concretes examined, significant amounts of the intruding sulfate accumulated near the top surfaces of the concretes where they were available to form gypsum. As a consequence, the microstructures of these concretes are characterized by zones of gypsum near the top and bottom surfaces, zones of ettringite adjacent to these, and central zones of monosulfate and Friedel's salt. The latter formed due to the ingress of chloride. Because of their high permeabilities, the use of sulfate-resisting cement alone was insufficient to protect these concretes from sulfate attack.

Keywords: Efflorescence; Ettringite; Friedel's salt; Gypsum; Sulfate attack

1. Introduction

Sulfate attack of concrete is a well-documented phenomenon. Sulfate attack associated with exposure to sulfate soils is well recognized in North America [1] and in the Arabian Gulf [2–4]. As such, the state of knowledge regarding the processes responsible for sulfate attack have been periodically reviewed. Notable among reviews are those by Thorvaldson [5], Swensen [6], and Mehta [7]. Consistent among these reviews and the extensive literature on the subject is the view that sulfate attack is caused primarily by the formation of ettringite and secondarily by that of gypsum.

It is generally recognized that sulfate ingress will result in concentration gradients in concrete [8]. An interesting example of this is a recent analysis of the distributions of sulfates in concretes exposed to a combination of sulfate soils and sulfates generated by the oil fires in Kuwait [9]. However, the effects of these gradients on the distributions of sulfate-containing phases in concretes exposed to sulfate soils do not appear to have been analyzed in any detail. In highly permeable concretes, these distributions are strongly influenced by the presence of evaporate fronts.

The proportion of sulfate added during cement manufacture is based on two factors. Sufficient sulfate must be present to avoid flash set. Alternatively, the proportion added must be less than that required for ettringite formation to continue to any substantial degree after the concrete has hardened. Thus, the average molar ratio of SO_3 to Al_2O_3 in Type I cement is 0.6 [10], although it may be higher in low C_3A cements. This ratio precludes the presence of gypsum in normal, mature concrete. The molar ratio of SO_3 to Al_2O_3 of 3 in ettringite also suggests that it should not be present after the cement paste has achieved a substantial degree of hydration. Rather, equilibrium considerations suggest the available sulfate should be present as monosulfate [11,12]. It is not abnormal, however, to observe some ettringite in mature concrete [13]. Occasionally, ettringite can be found to have recrystallized in locations, such as large air voids, where cyclic wetting and drying occur. Thus, a typical microstructure of normal concrete as viewed in polished

* Corresponding author. Tel.: +1-814-865-5352; fax: +1-814-863-7040.
E-mail address: etx@psu.edu (P.W. Brown).

0008-8846/00/$ – see front matter
PII: S0008-8846(00)00386-0

section by SEM will contain occasional ettringite in air voids. AFm and residual calcium aluminates will be distributed throughout the paste [13].

When concrete is subjected to an external source of sulfate, a variety of phenomena can occur. Assuming the concrete is relatively mature, the AFm and other aluminum-containing hydrates present convert to ettringite. In the event that the cation associated with the intruding sulfate is Na, K, or Mg, ettringite formation requires a supplementary source of calcium. Thus, the formation of ettringite decalcifies the cement paste according to reaction (1):

$$3CaO \cdot Al_2O_3 \cdot CaSO_4 \cdot 12H_2O + 2Ca(OH)_2 + 2Me_xSO_4 \xrightarrow{H_2O} 3CaO \cdot Al_2O_3 \cdot 3CaSO_4 \cdot 32H_2O + 2Me(OH)_y \quad (1)$$

if Me = Na or K, $x = 2$ and $y = 1$; if Me = Mg, $x = 1$ and $y = 2$.

If the cation is Na or K, $Me(OH)_y$ is NaOH or KOH. Because these are highly soluble, the pH increases as a result of decalcification. Alternatively, if Me is Mg, $Mg(OH)_2$ forms and the pH decreases. With the ingress of sufficient sulfate, available sources of alumina will be exhausted and additional ettringite cannot readily form. Gypsum forms instead. Because of the existence of sulfate concentration gradients, gypsum can be forming at one location while ettringite formation may still be occurring at another.

The reactions that may occur due to sulfate ingress are not limited to these well-documented phenomena. In the event of magnesium sulfate intrusion, Mg-containing compounds other than $Mg(OH)_2$ may form [14]. Depending on the rates of transport and the presence of evaporative surfaces, a portion of the alkali sulfates will pass through the concrete pore structure and produce effloresence at these evaporative surfaces. In addition, alkali sulfates may precipitate internally in the concrete.

This article documents the observation of these phenomena in field concretes subjected to sulfate attack. In particular, the observations made in the microstructural analyses of concretes from Southern California are summarized. The concretes studied exhibited high permeabilities and sodium, magnesium, sulfate, chloride, and carbonate were observed to have been transported deeply in their pore structures. In such highly permeable concretes, the distributions of sulfate- and chloride-containing solids may be complex when evaporative surfaces are present. Zones of deterioration and reaction fronts can be readily discerned. The microstructural features discussed in this article were consistently observed in slabs in contact with sulfate-containing ground water. In these instances, the distributions of ettringite and other sulfate-containing phases can be correlated with the movement of sulfate through the concrete pore structures and with the effects of surface evaporation. As is typical of crystallization processes, growth of existing crystals tends to be preferred over the nucleation of new crystals. Thus, additional ettringite is likely to form in locations where it is already present. Depending on the local conditions, additional ettringite forms in voids and in the paste.

Because ettringite forms in response to a compositional gradient in sulfate, it tends to exhibit non-uniform distributions. While the amount of ettringite observed might be expected to decrease with distance away from the surface in

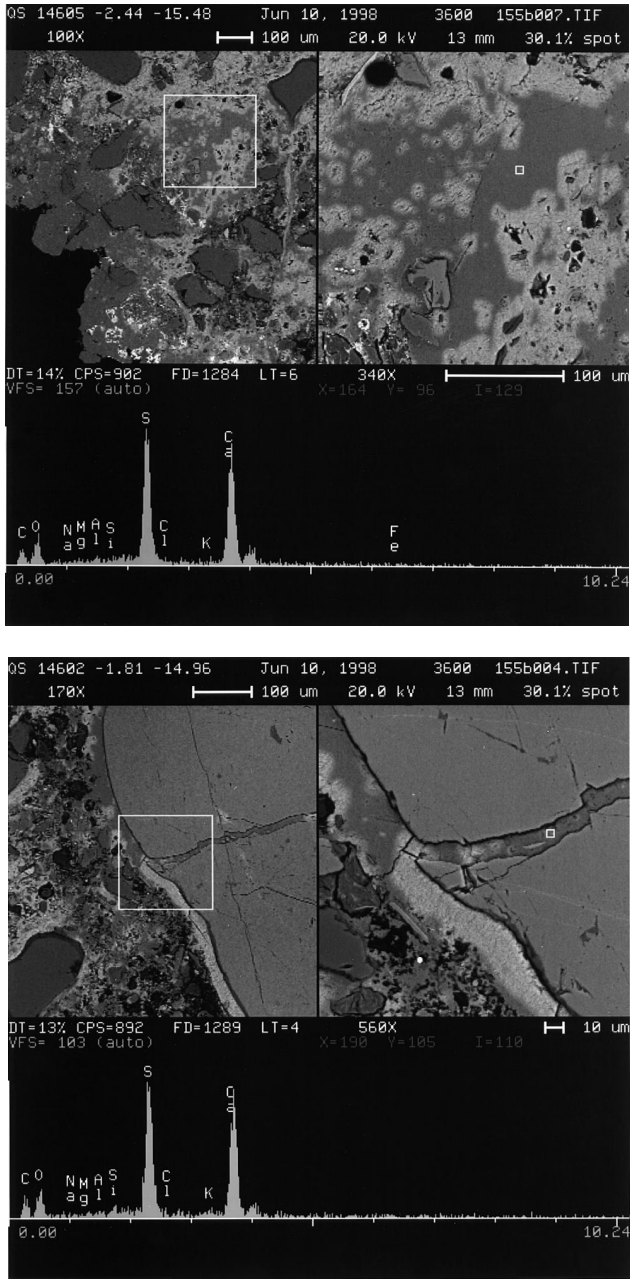

Fig. 1. (a) The microstructure of the region several millimeters thick near the bottom of the garage slab and the related EDS spectrum. The microstructure features reminiscent of normal cement paste are absent. Featureless gypsum entirely infills the regions in between fine aggregate. (b) Figure showing another region near the bottom surface of the slab where the gypsum has infilled a gap at the paste–aggregate interface and a crack in the aggregate.

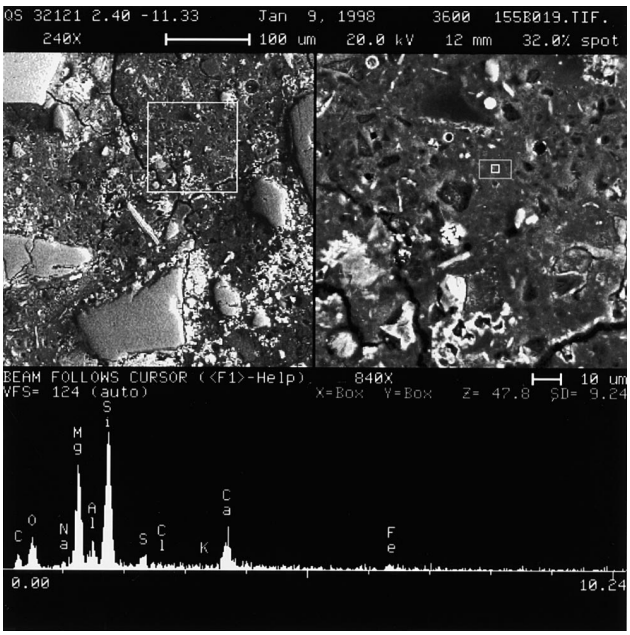

Fig. 2. The microstructure and the related EDS spectrum shows magnesium silicate (or an intimate mixture of brucite and silica gel) can also be observed in this region.

contact with the sulfate source, examination of field concrete slabs has shown this not to be the case. Ettringite formation was also observed near the top surfaces of the slabs, indicating that advection-based movement of sulfate can result in its formation at locations remote from the external sulfate source. Thus, the second purpose of this article is to describe the distributions of sulfate efflorescence, ettringite, AFm phases (sulfate and chloride), and gypsum. The mechanisms responsible for these distributions in concretes exposed to sulfate-containing ground water are also described.

2. Experimental

The concrete cores examined were obtained from a variety of locations in homes in Southern California. These included cores from interior slabs and garages. The concretes were constituted using Type II cement with fly ash or Type V cement and manufactured aggregate. The typical range of water-to-cement ratios was 0.65–0.70. Ratios in this range suggest the concretes to be highly permeable. The AASHTO rapid chloride permeability test [15] was carried out on these concretes and the results confirmed their high permeabilities [16].

The results of the present study rely primarily on the analyses of cores taken from garage slabs. This is because, full thickness cores could be removed from locations where the direction of sulfate transport is known. Coring garage slabs, where efflorescence could be readily observed on the slab surfaces, permits the correlation of the presence of efflorescence with the concrete microstructure.

The cores were sliced using a diamond wheel saw. Segments approximately 1 cm thick were taken along the length of the core. Each segment was about 50 mm in length and about 25 mm in width. One segment extended from the top surface to a depth of about 50 mm, the second was taken from the bottom of the slab to a height of about 50 mm. In some instances, a third segment was taken from the center of

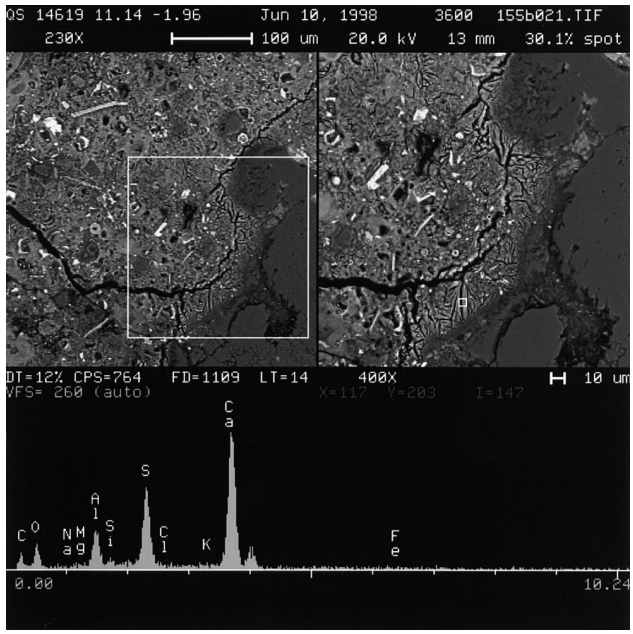

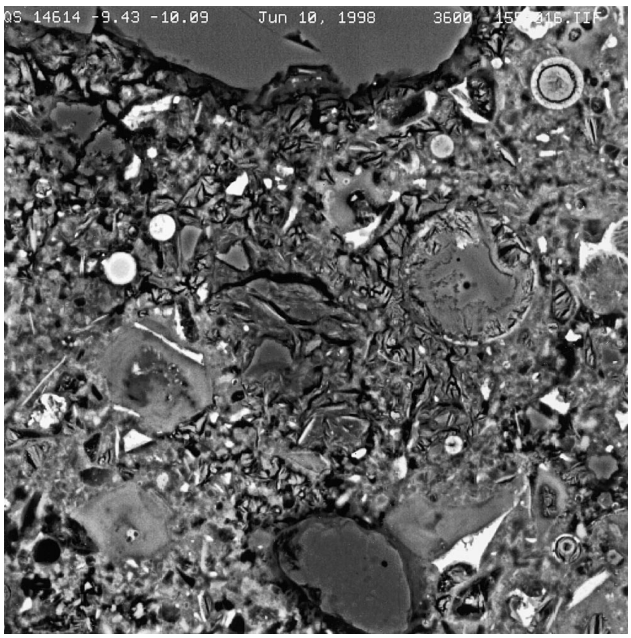

Fig. 3. (a) Ettringite filling the paste–aggregate interface and filling an air void. Ettringite formation at the paste–aggregate interface is consistent with the decalcification of the paste due to the ingress of the sodium sulfate/magnesium sulfate solution. (b) The formation of ettringite in the paste. This microstructure is typical of paste that is responding to the expansion associated with ettringite formation. The formation of a network of cracks with a spacing of 100–200 μm is also typical of the mechanical consequences of sulfate attack in the concretes examined.

the core. However, this was atypical because the slabs were normally about 4 in. or 100 mm thick. These slabs were dried and vacuum-impregnated with epoxy using a method described by Jakobsen et al. [17]. Thin sections were then prepared from these slabs in the usual manner [18] by diamond wheel sawing and polishing. After carbon coating, the distributions of Mg, Cl, and S in these thin sections were determined by *k* ratio analyses of microprobe data. Profiles across each thin section from the top of the core to the bottom were determined by measuring *k* ratios for each of these elements in fields approximately 70–90 μm in size. Averages of five fields each at about the same depths below the core surfaces were used to determine the relative abundances across each thin section. Determinations were carried out at ~4-mm increments across each thin section. The distributions of Mg, Cl, and S determined by the

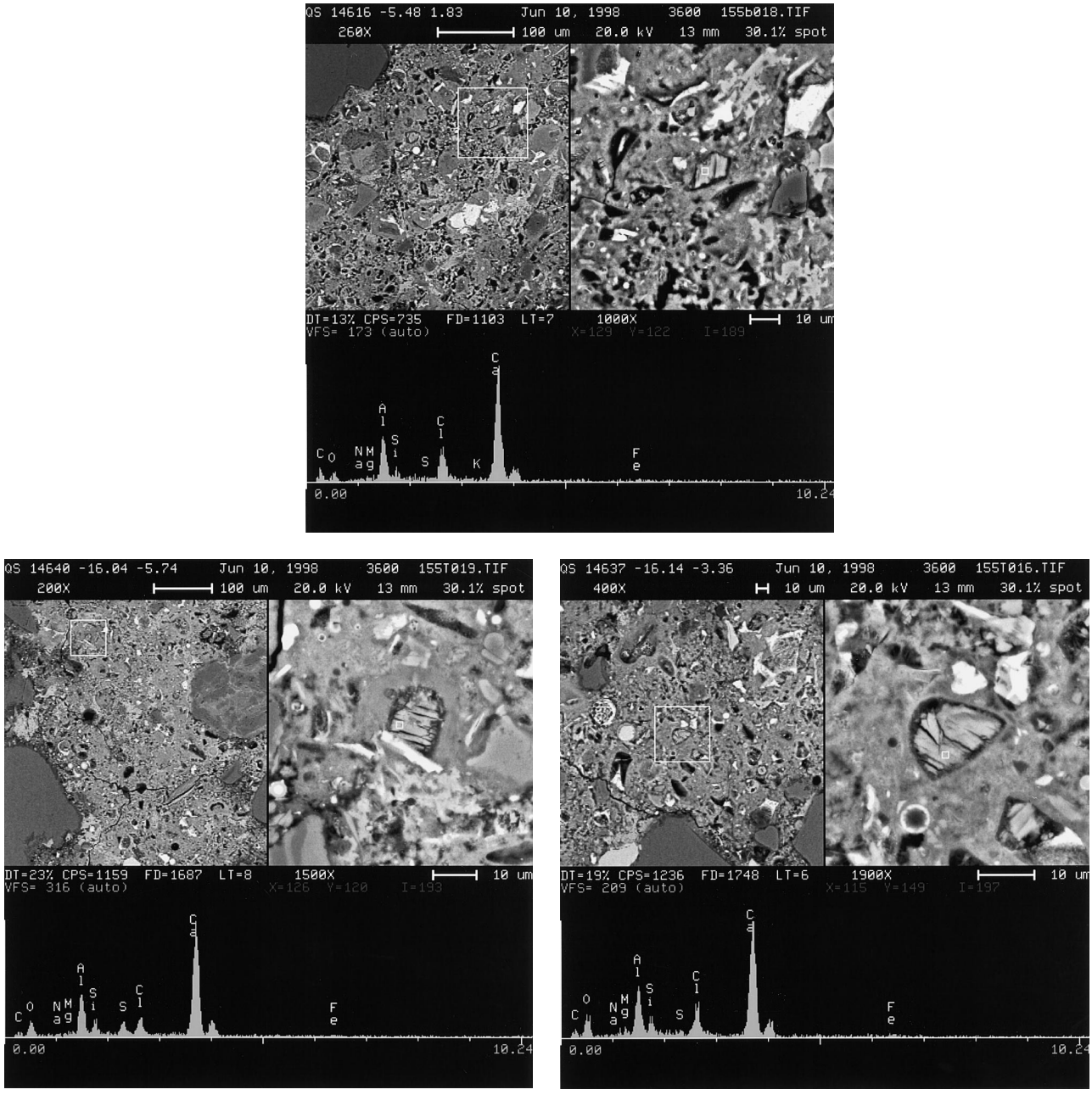

Fig. 4. (a) A microstructure and the related EDS spectrum of Friedel's salt. The relative heights of the chloride, aluminum, and calcium peaks in its EDS spectrum suggest this compound to be phase-pure Friedel's salt. The crystallization of ettringite at the paste–aggregrate interface can also be observed in this micrograph. (b) The morphology and EDS spectrum of a mixture of AFm phases. It is not unusual to observe compounds also containing sulfur and chloride which exhibit the same general morphology. (c) Friedel's salt near the top zone where it was observed. This figure illustrates that morphology of this compound remains nominally the same regardless of where it forms in the core and regardless of the presence of sulfate.

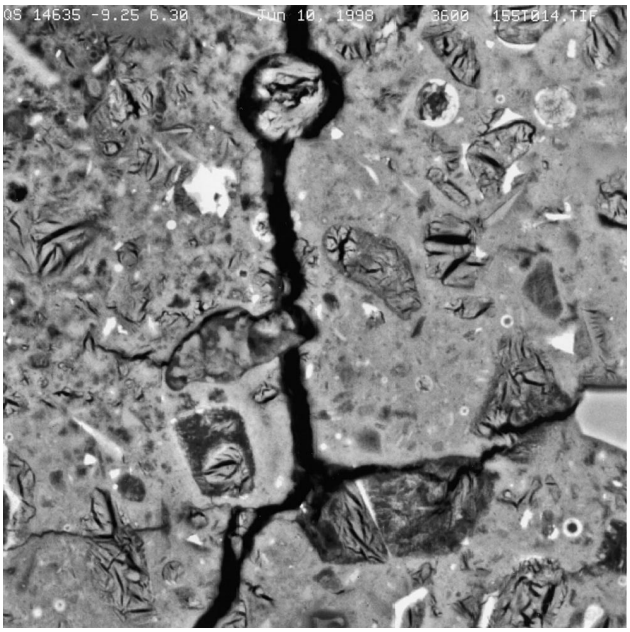

Fig. 5. Microstructure of ettringite, which has formed in the paste near the top surface of the concrete.

microprobe profiles were correlated with microstructural observations and with energy dispersive spectra of the microstructural features observed.

Phase-pure Friedel's salt was prepared by reacting tricalcium aluminate with calcium chloride at room temperature at a liquid-to-solids ratio of about 10. The tricalcium aluminate was prepared by firing a 3:1 molar ratio mixture of $CaCO_3$ and alumina at 1250°C for 4 h followed by hand grinding to a particle size of approximately 15 μm. This Friedel's salt was reacted with a sodium sulfate solution under conditions where the SO_3/Al_2O_3 ratio of the system exceeded 3. After reaction for approximately 2 h, the slurry was filtered and solids present were dried. The phases present were determined by X-ray diffraction analysis.

3. Results and discussion

The following series of micrographs were obtained from a garage slab on which the presence of effloresence was detected. This core was selected for study in detail because it was obtained from a location within the garage of a home approximately 9 years old, where exposure to rain and direct sunlight were unlikely. Fig. 1a shows the microstructure of the region several millimeters thick near the bottom of the garage slab and the related EDS spectrum. Notable is the absence of microstructural features reminiscent of normal cement paste. Essentially, the only feature observed is that of relatively structureless gypsum entirely infilling the regions in between fine aggregate. Fig. 1b shows another region near the bottom surface of the slab. This micrograph shows the gypsum has infilled a gap at the paste–aggregate interface and has infilled a crack in the aggregate. The formation of magnesium silicate (or an intimate mixture of brucite and silica gel) can also be observed in this region. This is shown in Fig. 2. Although the microstructure does not appear unlike that of normal cement paste, the calcium is virtually absent and has been replaced by Mg. Such an observation was not unique to the specimen shown in Fig. 2 and the formation of magnesium silicates in concrete sub-

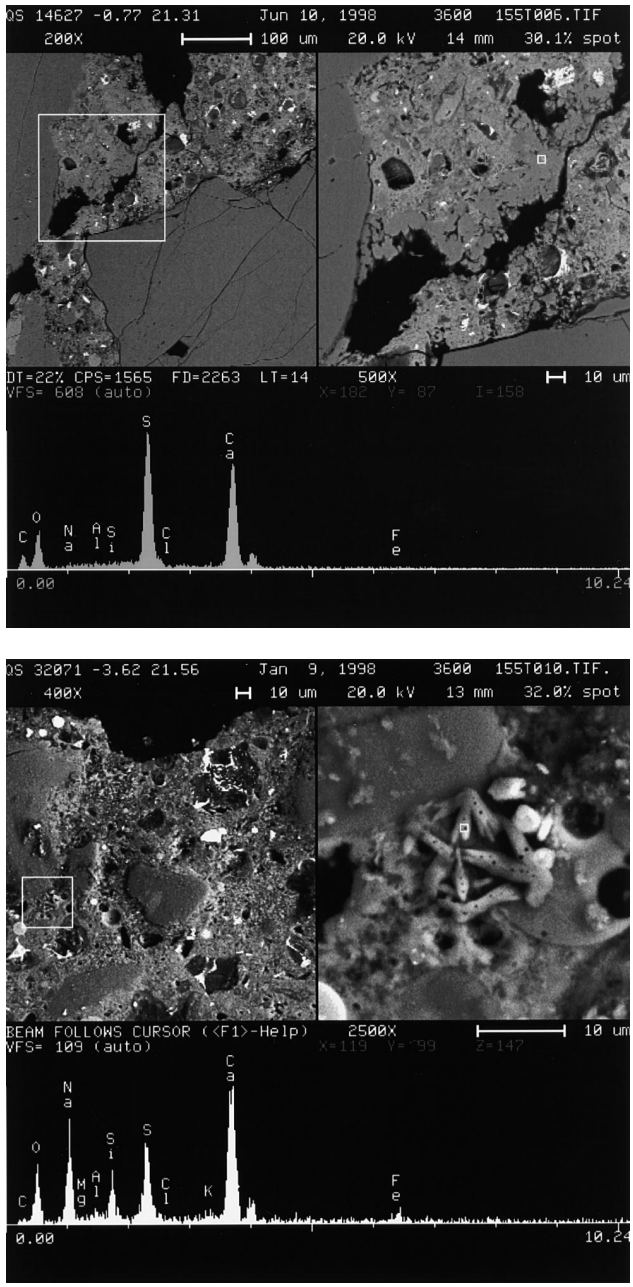

Fig. 6. (a) Microstructure and the related spectra from the near-surface region showing a second zone of gypsum that has crystallized. (b) Microstructure and EDS spectrum of sodium sulfate that has crystallized near the top surface of the concrete. The Si and Al peaks result from the underlying piece of aggregate.

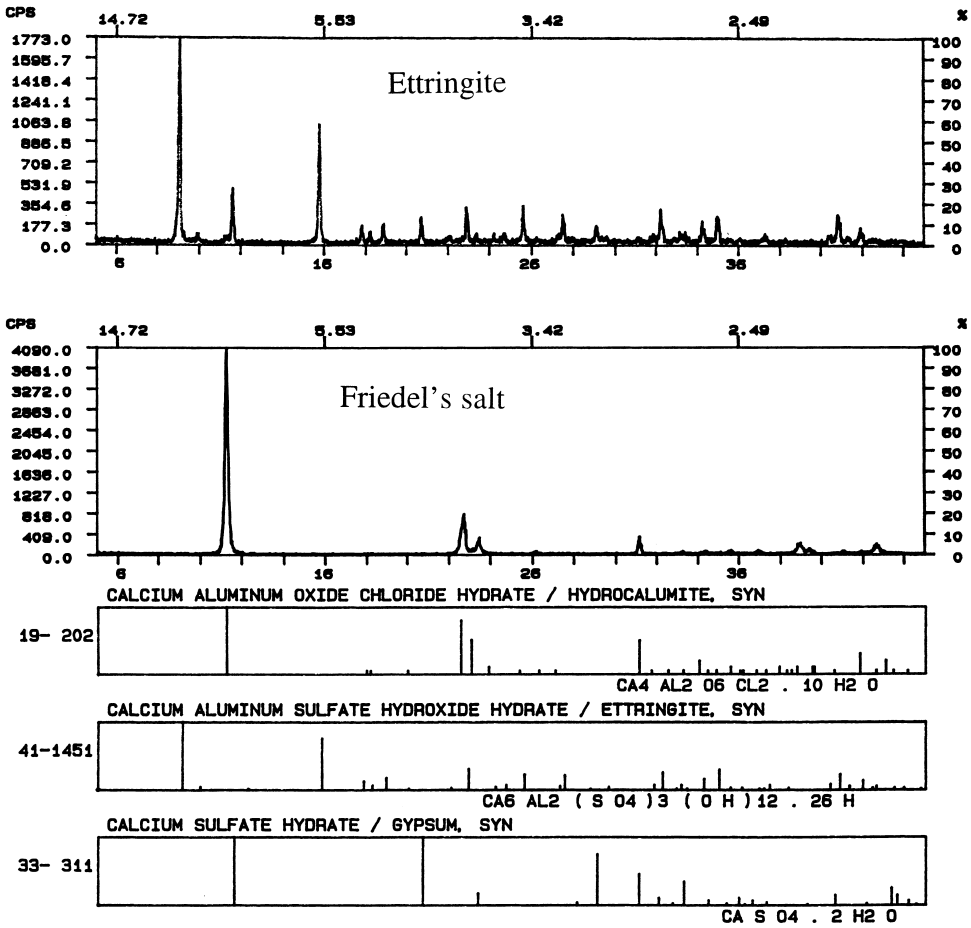

Fig. 7. The X-ray diffraction patterns obtained before and after Friedel's salt was exposed to sodium sulfate solution indicating that it converts to ettringite.

jected to magnesium sulfate attack has been discussed elsewhere [14].

It was typical to observe gypsum in these concretes. The presence of gypsum and magnesium silicate is consistent with a mechanism in which Mg was transported as the $MgSO_4^0$ neutral species to the sites where it reacted [14]. As local regions of high pH, such as those near anhydrous cement grains or $Ca(OH)_2$ were encountered, the following reactions (Reactions (2) and (3)) occurred leading to the distributions of solids observed:

$$Ca(OH)_2 + MgSO_4^0 \overset{H_2O}{\Rightarrow} CaSO_4 \cdot 2H_2O + Mg(OH)_2 \quad (2)$$

$$x\mathrm{Mg(OH)}_2 + y\mathrm{Si(OH)}_z \overset{H_2O}{\Rightarrow} x\mathrm{MgO}\cdot y\mathrm{SiO}_2\cdot n\mathrm{H}_2\mathrm{O} \quad (3)$$

Thus, a phase assemblage comprised of gypsum and magnesium silicate indicates that concrete in this region had reached an end state of deterioration and further chemical change is unlikely.

Analysis of the microstructures and compositions of the solids formed at locations in the core more remote from ground contact revealed that ettringite had formed. A zone of ettringite formation approximately 20 mm thick had formed above the gypsum layer and extensive cracking had occurred. Typical microstructures are shown in Fig. 3a and b. Fig. 3a shows ettringite filling a paste–aggregate interfacial region. Formation of ettringite at the paste–aggregate interface was commonly observed. This is consistent with the decalcification due to sulfate attack as expressed in Reaction (1) and would be expected in concrete undergoing sulfate attack. One consequence of this is the loss of $Ca(OH)_2$ from the paste–aggregate interfaces. Thus, the formation of ettringite at the paste–aggregate interface is consistent with the decalcification of the paste due to the ingress of sodium sulfate and/or magnesium sulfate solutions.

Fig. 3b shows the formation of ettringite in the paste. Although this concrete was cast at a water-to-cement ratio of about 0.7 [19], the undifferentiated paste in this region was relatively dense. This is typical of paste in which ettringite had formed. The formation of networks of cracks with a spacing of 100–200 μm (Fig. 3a) was also typical.

At greater distances from the bottom of this core, ettringite formation was observed less frequently. Rather, the aluminate-containing phases present were monosulfate or Friedel's salt. Fig. 4a shows a microstructure and the related EDS spectrum of the latter. It was not atypical to

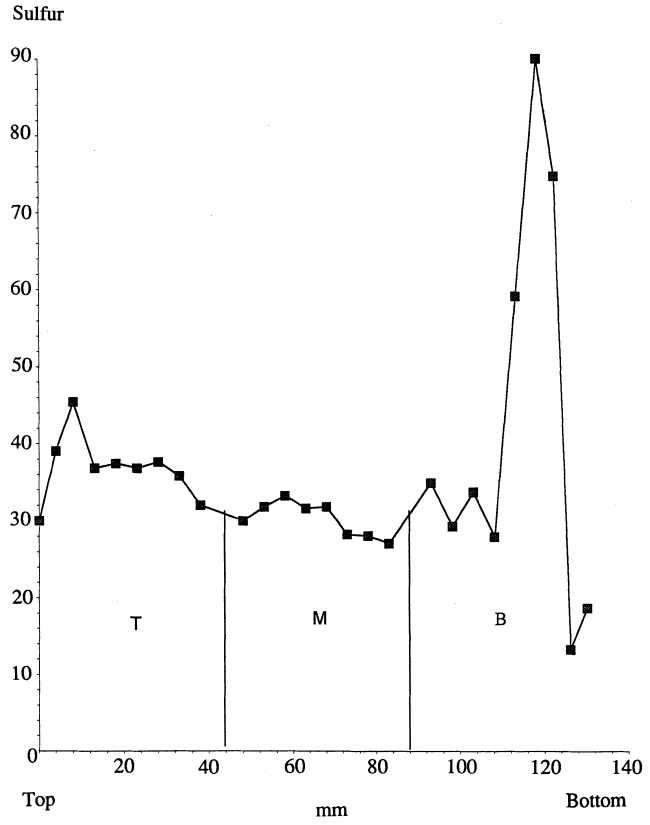

Fig. 8. The distribution of sulfate in concrete as determined by microprobe analysis showing it to be consistent with the phase assemblages observed.

observe Friedel's salt in association with the ferrite phase (bright grains in the micrograph) as shown. Chloride is also capable of reacting with ferrite to form the iron analog of Friedel's salt [20]. Based on the relative heights of the chloride, aluminum, and calcium peaks in its EDS spectrum, the compound shown in Fig. 4a is phase-pure Friedel's salt. However, it was not unusual to observe compounds also containing sulfur but exhibiting the same general morphology as Friedel's salt. Fig. 4b shows the morphology and EDS spectrum in such an instance. This is assumed to be an assemblage of monosulfate and Friedel's salt. Friedel's salt or mixtures with monosulfate were observed in a zone throughout the central region of this concrete extending to about 22 mm from the top of this core. Ettringite was only occasionally present in this region. Fig. 4c shows Friedel's salt near the top of this zone. This figure illustrates the morphology of this compound remained nominally the same regardless of where it formed in the core and regardless of the presence of sulfate. The presence of Friedel's salt throughout this region is indicative of the alteration of the paste due to the intrusion of chloride.

As the top surface of this concrete is approached, Friedel's salt and monosulfate were no longer observed. Rather, a second zone of ettringite formation was present. This zone was approximately 12 mm thick. Thus, the zone of Friedel's salt and monosulfate is sandwiched between two zones of ettringite. Fig. 5 illustrates ettringite in the paste in this zone.

Above this second zone of ettringite is the near-surface region where gypsum and other forms of sulfate-based efflorescence were observed. Fig. 6a is in the region where gypsum had crystallized and Fig. 6b shows a region where sodium sulfate had crystallized. Visual inspections of concrete from homes in Southern California indicate the appearance of efflorescence to be a common phenomenon. Prior studies have shown that it was not unusual to observe efflorescence on concrete surfaces [14,21,22]. Slab-on-grade over relatively shallow perimeter footings is typical of residential construction in the region. Low relative humidity and temperate climate create conditions favoring the rapid transport of ground water through permeable concrete.

The zonal formation of various compounds indicative of the ingress of aggressive species from the ground water is evident in the microstructure of this concrete. The zone of gypsum near the bottom of the core lies beneath a zone where ettringite formation was extensive. This assemblage is consistent with the literature on sulfate attack. However, extensive ettringite formation was also commonly observed in the absence of a gypsum zone. The presence of a zone in which chloride AFm was routinely observed but where ettringite was only occasionally present is phenomenologically interesting and raises the question as to the relative stabilities of these compounds. To establish their relative stabilities, Friedel's salt was reacted with a sodium sulfate solution under conditions where the SO_3/Al_2O_3 ratio of the system exceeded 3. Fig. 7a shows the diffraction pattern of Friedel's salt prior to exposure to sodium sulfate solution. Fig. 7b shows the diffraction patterns of the solids present after exposure. Reference patterns of relevant solids are shown for comparison. These data indicate that the Friedel's salt had converted to ettringite in the presence of a sodium sulfate solution. Thus, ettringite is the stable phase under these conditions.

The presence of a zone of ettringite, gypsum, and sodium sulfate above the zone of the Friedel's salt indicates that sulfate had passed through the region where Friedel's salt had formed. The above stability relationship suggests that Friedel's salt persists because the rate of sulfate transport across this zone was higher than its rate of reaction to form ettringite, not because Friedel's salt is stable with respect to ettringite. The stability relationship observed indicates this zone of Friedel's salt will diminish in thickness as the ettringite zones expand.

In a broad sense, the distributions of phases in the concretes studied were symmetrical. There were zones of monosulfate and Friedel's salt in the central region of the cores. These were sandwiched in between zones of ettringite with zones of gypsum surrounding the ettringite. These distributions indicate the presence of sulfate gradients in the concrete from the surfaces inward. One distribution of

sulfate as determined by microprobe analysis is presented in Fig. 8. This figure shows the sulfate distribution across the core to be in accord with the sulfate contents of the phase assemblages observed. The accumulation of gypsum near the bottom of this core was the result of the availability of sulfate in the ground water. The accumulation of gypsum near the top surface of the concrete was the result of sodium sulfate transport through the pore structure and its conversion to gypsum in that region. Both processes occurred according to Reaction (4):

$$Na_2SO_{4(aq)} + Ca(OH)_2 \overset{H_2O}{\Rightarrow} CaSO_4 \cdot 2H_2O + 2NaOH_{(aq)} \quad (4)$$

4. Summary

The movement of sulfate through the concretes analyzed resulted in three forms of sulfate attack: salt crystallization, ettringite formation, and gypsum formation. Although sulfate-resisting cement was used, that alone was insufficient to confer sulfate resistance to the concretes examined. Sulfate resistance may be imparted to concrete by limiting the C_3A content of the cement, by controlling the permeability of the concrete, or both. The microstructural evidence presented supports the views of Verbeck [23] and Mehta [7] that control of permeability is more important than cement composition in achieving sulfate-resistant concrete.

Acknowledgment

We gratefully acknowledge the help of Jason O'Hern in micrograph preparation.

References

[1] F.R. MacMillan, T.E. Stanton, I.L. Tyler, W.C. Hansen, Long-Time Study of Cement Performance in Concrete: Chapter 5. Concrete Exposed to Sulfate Soils, ACI Spec. Publ., Detriot, 1949 (64 pp.).
[2] W.C. Rasheeduzzafar, F.H. Dakhil, A.S. Al-Gahtani, S.S. Al Saadoun, M.A. Bader, Influence of cement composition on the corrosion of reinforcement and sulfate resistance of concrete, ACI Mater J 87 (1990) 114–122.
[3] Z.G. Matta, Deterioration of concrete structures in the Arabian Gulf, Concr Int 15 (1993) 33–36.
[4] O.S.B. Al-Amoudi, M. Maslehuddin, M.M. Saadi, Effect of magnesium sulfate and sodium sulfate on the durability performance of plain and blended cements, ACI Mater J 92 (1995) 15–24.
[5] T. Thorvaldson, Chemical aspects of durability of cement products, 3rd ICCC, Cement and Concrete Association, London, 1952, pp. 436–485.
[6] E.G. Swensen (Ed.), Performance of Concrete, Univ. of Toronto Press, Toronto, 1968.
[7] P.K. Mehta, Sulfate attack on concrete — a critical review, in: J.P. Skalny (Ed.), Materials Science of Concrete, Am. Ceram. Soc., Westerville, 1992, pp. 104–130.
[8] R.W. Day, Damage to concrete flatwork from sulfate attack, J Perform Constr Facil 9 (1995) 302–310.
[9] H. Al-Khaiat, Effects of pollution from Kuwait oil well fires on concrete properties, ACI Mater J 96 (1999) 109–115.
[10] H.M. Kanare, E.M. Gartner, Optimum sulfate in Portland cement, Cements Research Progress 1984, Am. Ceram. Soc., Westerville, 1985, p. 213.
[11] P.W. Brown, The hydration of tricalcium aluminate and tetracalcium aluminoferrite in the presence of calcium sulfate, Mater Struct 19 (110) (1986) 137–147.
[12] P.W. Brown, The implications of phase equilibria on hydration in the tricalcium silicate–water and the tricalcium aluminate-gypsum-water systems, 8th ICCC, Rio de Janeiro, Finep; Rio, 3 (1986) 231–239.
[13] H.F.W. Taylor, Cement Chemistry, Academic Press, London, 1990.
[14] P.W. Brown, A. Doerr, Chemical changes in concrete due to the ingress of aggressive species, Cem Concr Res 30 (2000) 411–418.
[15] Standard Method of Test for Resistance of Concrete to Chloride Ion Penetration, AASHTO Designation T 259-80, 1990; ASTM Designation C 1202-97 Standard Test Method for Electrical Indication of Concrete's Ability to Resist Chloride Ion Penetration.
[16] N. Hearn, private communication (1997).
[17] U.H. Jakobsen, V. Johansen, N. Thaulow, Estimating the cappilary porosity of cement paste by fluorescent microscopy and image analysis, in: S. Diamond, S. Mindess, F. Glasser, L. Roberts, J. Skalny, L. Wakely (Eds.), Microstructure of Cement-Based Systems/Bonding and Interfaces in Cementitious Materials, MRS Symp Proc, 370 (1995) 226–236.
[18] ASTM Designation C856-95, Standard Practice for Petrographic Examination of Hardened Concrete.
[19] N. Thaulow, private communication (1998).
[20] A.K. Suryavanshi, J.D. Scantlebury, S.B. Lyon, The binding of chloride ions by sulphate resistant Portland cement, Cem Concr Res 25 (1995) 581–592.
[21] G.A. Novak, A.A. Coleville, Efflorescent mineral assemblages associated with cracked and degraded residential concrete foundations in Southern California, Cem Concr Res 19 (1989) 1–7.
[22] B.C. Yen, R.E. Bright, Residential Foundation Deterioration Study for the Cities of Lakewood, La Palma and Cypress, California, California State University, Fullerton, 1990.
[23] G.J. Verbeck, Field and laboratory studies of the sulphate resistance of concrete, in: E.G. Swensen (Ed.), Performance of Concrete, Univ. of Toronto Press, Toronto, 1968, pp. 113–124.